Volume 14 Issue 1 (2026) pp. 90-103 **DOI**: 10.48309/IJABBR.2026.2065708.1635

Original Article

Structural Insights and Binding Site Analysis for Improved CRISPR-Cas13a Sensitivity and Efficiency

Zahra Ghanei

Department of Biotechnology, Faculty of Biological Sciences, Alzahra University, Tehran, Iran

*Corresponding Author E-mail: Z.Ghanei@alzahra.ac.ir

Submitted: 2025-07-13, Revised: 2025-08-12, Accepted: 2025-09-22

Abstract

CRISPR-Cas13a systems have revolutionized RNA detection and manipulation, with trans-cleavage activity playing a pivotal role in their diagnostic applications. Enhancing this activity is crucial for achieving greater sensitivity, speed, and versatility in both research and clinical settings. Targeting specific protein binding sites with organic chemical agents represents a promising approach for increasing trans-cleavage activity. This research utilized homology modelling alongside computational approaches, including InterProSurf, GHECOM, and eF-seek, to examine structural characteristics and identify high-confidence binding sites in Cas13a orthologs. These methods provided a comprehensive analysis of the protein's functional architecture, contributing to a deeper understanding of its mechanistic behaviour. Functional amino acids located on the protein surface, along with pockets exhibiting lower binding affinity scores, were identified as potential binding sites for small molecules. Key residues influencing ligand interactions were pinpointed, including residues 603, 605, and 606 in LbaCas13a; residues 1112 and 1145 in LbuCas13a; and residues 735, 784, and 787 in LshCas13a. The eF-seek analysis revealed more extensive residue interaction networks in LbaCas13a, which correlate with its enhanced trans-cleavage activity. These findings provide a comprehensive framework for optimizing CRISPR-Cas13a systems, offering valuable insights for improving their sensitivity and efficiency in precision diagnostics. Future research can refine Cas13a-based tools by focusing on their structural and functional details to unlock their full potential in biomedical applications.

Keywords: Cas13a, CRISPR/Cas detection, Trans-cleavage, Binding site, Bioinformatics.

Introduction

CRISPR-Cas systems are adaptive immune mechanisms in prokaryotes that recognize and cleave foreign nucleic acids [1,2]. These systems are broadly classified into Class 1 (multi-subunit effector complexes) and Class 2 (single-protein effectors). Class 2 systems, including Cas9, Cas12, and Cas13, are widely repurposed for molecular diagnostics due to their programmable RNA/DNA targeting and collateral cleavage activity [3,4]. Cas9 functions by binding and cleaving double-stranded DNA (dsDNA) guided by RNA (gRNA), but it does not possess collateral activity. In contrast, Cas12 targets both dsDNA and single-stranded DNA (ssDNA) and demonstrates trans-cleavage of non-target ssDNA.

Uniquely, Cas13 targets RNA and exhibits trans-cleavage of RNA. The Cas12 and Cas13 form the basis of nucleic acid detection in systems such as DETECTR (for DNA) and SHERLOCK (for RNA), enabling highly sensitive diagnostic applications [5-7].

The current CRISPR-based diagnostic platforms utilizing Cas12 and Cas13 effectors have shown robust capabilities for multiplex detection of diverse viral and bacterial pathogens [8-10]. While effective, these systems generally require nucleic acid pre-amplification (*e.g.,* RPA or PCR), introducing workflow complexity. Strategic enhancement of trans-cleavage activity emerges as a critical optimization approach, offering dual advantages: (1) elimination of pre-amplification requirements, significantly reducing time to result, and (2) improved suitability for point-of-care testing (POCT) applications through simplified operational workflows [11,12].

CRISPR-Cas13a (formerly C2c2) is an RNA-guided RNA-targeting effector protein that exhibits trans-cleavage activity, enabling it to degrade non-target RNA molecules upon activation. Cas13 comprises two HEPN (Higher Eukaryotes and Prokaryotes Nucleotide-binding) domains responsible for RNA cleavage. Target RNA binding induces HEPN domain activation and crRNA-target RNA duplex formation stabilized by a positively charged groove [6,7,13].

Recent advances in computational chemistry and bioinformatics offer a promising avenue to enhance Cas13a's trans-cleavage by identifying small-molecule modulators that stabilize its active conformation [12,14-16]. Structural analyses have revealed transient pockets that undergo significant conformational changes during RNA binding and cleavage processes. Beyond the immediate active site, computational predictions have identified distal regulatory hotspots that could serve as potential targets for chemical modulation of trans-cleavage activity [17-20]. In this study, we conducted a comprehensive structural analysis of Lachnospiraceae bacterium Cas13a (LbaCas13a), Leptotrichia buccalis Cas13a (LbuCas13a) and Leptotrichia shahii Cas13a (LshCas13a), performing comparative evaluations with other Cas13a orthologs to identify evolutionarily conserved residues. Through systematic examination of functional protein surfaces, we mapped potential catalytic pockets and ligand-binding sites using computational approaches. Key residues implicated in molecular interactions were further validated through consensus analysis across multiple bioinformatics tools, with selected sites prioritized for subsequent functional characterization and binding analysis.

Methods

Sequence Availability, Blast, and Conserved Domains Search

The protein sequences of LbaCas13a (Accession: 5W1I), LbuCas13a (Accession: 5XWY), and LshCas13a (Accession: 7DMQ) were retrieved from NCBI's protein database and stored in FASTA format for subsequent examination [17]. These sequences were then employed as search queries in BLAST (Basic Local Alignment Search Tool) to compare against the comprehensive non-redundant protein database available through NCBI's BLAST interface [18]. Furthermore, potential conserved domains within these protein sequences were investigated using the same NCBI platform's domain search functionality.

PSI-BLAST and COBALT Alignment

The protein sequences of LbaCas13a, LbuCas13a, and LshCas13a served as queries for PSI-BLAST (Position-Specific

Iterated BLAST) searches against the Protein Data Bank (PDB) through NCBI's BLAST interface [18]. This analysis aimed to identify structurally homologous proteins in the PDB database. For comprehensive homology assessment, the corresponding Cas13a sequences were retrieved from the RefSeq database as reference datasets.

Homology Modelling and Structure Assessment

The three-dimensional structure of LbaCas13a was predicted through homology modelling using SWISS-MODEL, a web-based protein structure prediction service [19]. The modelling process involves four key steps: template identification, target-template alignment, model-building, and quality evaluation. These steps rely on specialized computational methods and integrate current protein sequence and structure databases. The workflow is iterative, allowing refinement until satisfactory results are achieved. SWISS-MODEL's structure assessment service combines multiple validation tools with sequence and structure visualization to facilitate model evaluation. The assessment can be performed independently or by comparison with a reference structure, enabling detailed analysis of model quality and structural features. The GMQE (Global Model Quality Estimation) score in SWISS-MODEL predicts the overall quality of protein structural models generated via homology modelling, ranging from 0 to 1, with 1 indicating highest confidence. QMEANDisCo Global integrates local and global structural features for a comprehensive quality assessment.

Protein Structural Similarity

The structural similarity between the Cas13a proteins was evaluated using TM-align (Template Modelling Alignment tool) [20], which calculates two key metrics: the Root-Mean-Square Deviation (RMSD) and the TM-score, ranging from 0 to 1. Proteins with a TM-score above 0.5 are typically considered to share the same fold, while those with a TM-score below 0.5 are less likely to exhibit similar folding patterns. Additionally, a TM-score below 0.17 indicates that the proteins are structurally unrelated.

Interfaces Prediction

For comprehensive protein surface characterization, the InterProSurf computational tool was implemented [21]. InterProSurf was utilized to predict functional sites through its advanced patch analysis methodology, which systematically evaluates surface properties to identify potential interaction regions.

Pockets Detection

Complementing this approach, GHECOM (Grid-based HECOMi finder), was employed to detect and analyse multi-scale binding pockets using mathematical morphology techniques [22]. This method provides a distinct yet valuable perspective by focusing on cavity identification across various size scales.

Ligand Binding Site Prediction

The functional characterization of LbaCas13a, LbuCas13a, and LshCas13a proteins incorporated structural analysis through eF-seek, a specialized web server for ligand binding site prediction [23]. This approach leverages the fundamental principle that protein molecular function emerges from three-dimensional structure, where structural similarities often correlate with functional relationships.

eF-seek operates by comparing uploaded PDB-format protein structures

against its comprehensive eF-site database using an advanced clique search algorithm. This methodology identifies potential ligand interaction sites by detecting structural similarities with known binding pockets from characterized proteins. The analytical framework of the platform proves particularly valuable for studying RNA-targeting proteins such as Cas13a variants, where small molecule interactions may modulate nuclease activity or guide RNA binding.

Results

PDB and Conserved Domain Search

A BLAST search of the Protein Data Bank (PDB) returned several hits. The highest-scoring results were LbaCas13a (Chain A, LbaCas13a H328A (C2c2) [Lachnospiraceae bacterium NK4A179, 99.93% % identity, 100% query coverage), LbuCas13a (type VI-A CRISPR-associated RNA-guided ribonuclease Cas13a [Leptotrichia buccalis], 99.83% identity, 100% query coverage), and LshCas13a (Chain A, CRISPR-associated endoribonuclease C2c2 [Leptotrichia shahii DSM 19757], 98.92% % identity, 100% query coverage). The illustration of conserved domains detected in Cas13a variants is shown in Figure 1. Cas13a enzymes can be categorized into two distinct types based on their cleavage preferences: adenosine (A) cleaving and uridine (U) cleaving. Among these, LbaCas13a specifically targets adenosine (A), while the other two variants, LbuCas13a and LshCas13a, are known for their uridine (U) cleavage activity. A conserved motif characterized by the residue pattern R-N-H-R-[KDN]-H has been identified as essential for enzymatic activity.

Sequence Alignment

To analyze homology, the protein sequences of LbaCas13a, LbuCas13a, and LshCas13a were retrieved from the RefSeq database. Multiple sequence alignment was conducted using COBALT, a progressive alignment tool.

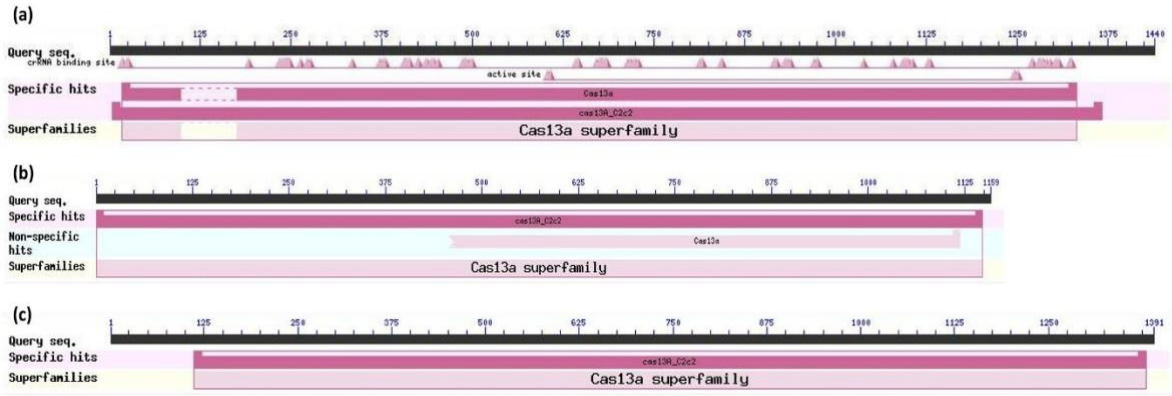

Figure 1 Illustration of conserved domains detected in (a) LbaCas13a, (b) LbuCas13a, and (c) LshCas13a

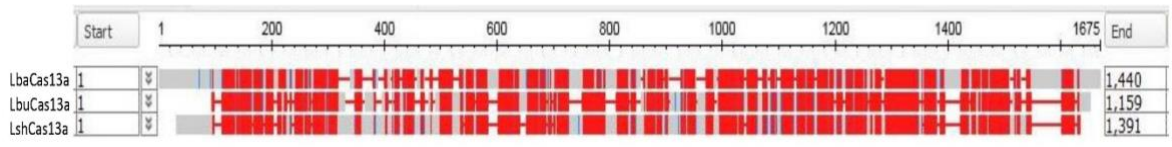

Figure 2 Illustration of alignment results with conservation color scheme in Cas13a variants

COBALT employs pairwise constraints derived from three primary sources: conserved domain databases (via RPS-BLAST), protein motif databases (via BLASTP), and local sequence similarity (via PHI-BLAST). To optimize computational efficiency, COBALT clusters sequences with a high number of shared words and identifies conserved domains and motifs for only one representative sequence per cluster. The alignment results are depicted in Figure 2, using a color scheme based on relative entropy to represent amino acid conservation. In this scheme, red indicates high conservation, while blue signifies low conservation.

Homology Modelling and Structure Assessment

The Swiss model predicted two models for LbaCas13a, three for LbuCas13a, and three for LshCas13a. Models with the highest GMQE and QMEANDisCo scores were selected, ensuring a moderate to high QMEAN Z-score and favorable Ramachandran plot outcomes. The selected models for LbaCas13a, LbuCas13a, and LshCas13a demonstrated the following quality scores: LbaCas13a had a GMQE of 0.9 and a QMEANDisCo global score of 0.89 ± 0.05, LbuCas13a had a GMQE of 0.87 and a QMEANDisCo score of 0.84 ± 0.05, and LshCas13a had a GMQE of 0.77 and a QMEANDisCo score of 0.72 ± 0.05. Figure 3 illustrates the highest-scoring models, with QMEANDisCo, a composite scoring function, estimating per-residue quality by combining single-model metrics with data from homologous experimental structures. Residues scoring below 0.6 in the "Local Quality" plot are identified as potentially inaccurate. Additionally, Figure 4 displays Ramachandran plots, mapping energetically favorable dihedral angles of amino acid backbones to validate structural plausibility.

TM-align Structural Alignment

Structural alignment performed using TM-align revealed that the variants maintained a TM-score greater than 0.5, indicating a high confidence in shared protein fold. However, the high RMSD values observed in these samples suggested that the proteins might adopt different folds or conformations. Notably, even in cases where RMSD is elevated, a TM-score approaching 1 can still signify functional or evolutionary relationships, a finding that aligns with the examples observed in our study (Table 1).

Interfaces Prediction

InterProSurf results show functional sites on protein structure surface. These results indicate that 110, 111, 112, 113, and 114 residues are the most functionally relevant in the lbaCas13a, while residues 860, 861, 863, 864, 865, 866, 867, 857, 858, 1215, 1216, 1217, and 1218 are relevant in the LshCas13a structure. For LbuCas13a, no amino acids were identified. Functional residues at the protein surface structures predicted by InterProSurf are indicated in Table 2.

Pockets Detection

GHECOM server finds five pockets on LbaCas13a, LbuCas13a, and LshCas13a surfaces using mathematical morphology. In this regard, GHECOM computes a pocket score (sum of 1/[Rpocket] /(1/[Rmin]*[vol of shell])) for each residue. A residue in a deeper and larger pocket has a larger value of pockets. The pockets of small-molecule binding sites and active sites were higher than the average value; specifically, the values for the active sites were much higher. This suggests that pockets contribute to the prediction of binding sites and active sites from protein structures.

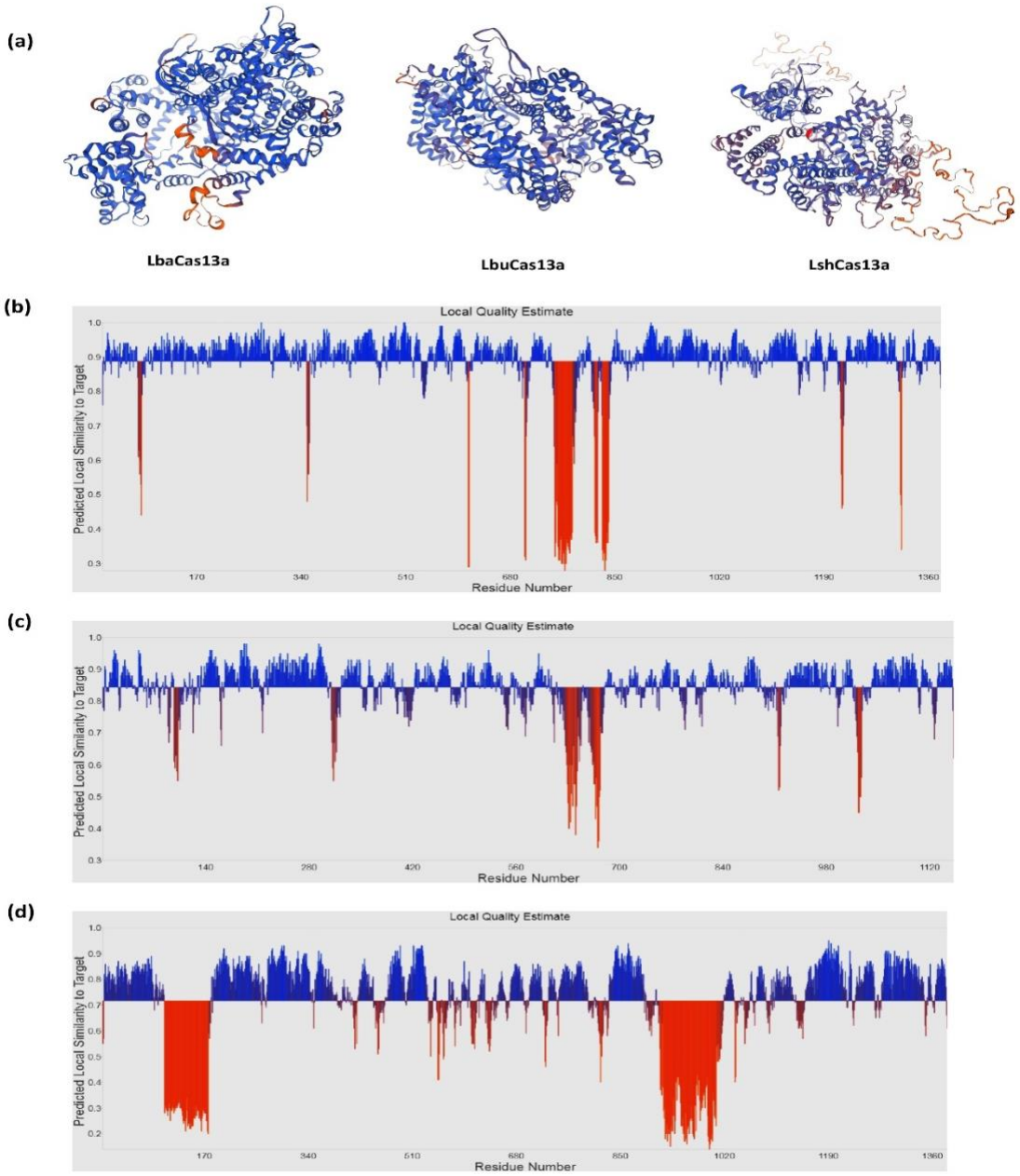

Figure 3 SWISS-MODEL predictions. (a) LbaCas13a, LbuCas13a and LshCas13a 3D structures based on confidence color scheme (residues are colored by their local quality value). (b) The "Local Quality" plot for each residue of the model (reported on the x-axis), and the expected similarity to the native structure (y-axis)

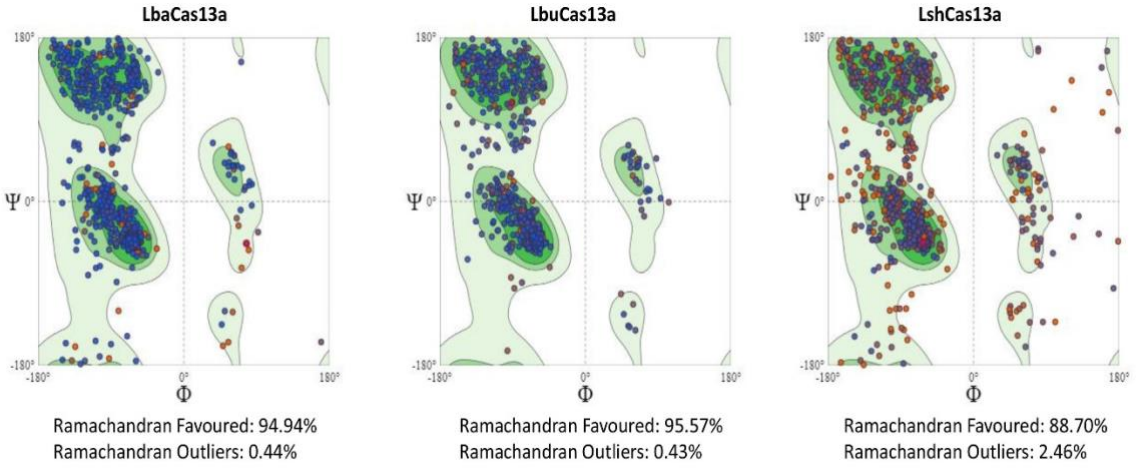

Figure 4 Ramachandran plot of predicted models for LbaCas13a, LbuCas13a, and LshCas13a

Table 1 TM align analysis of Cas13a variant models

Template	Sample	RMSD	TM-score
LbaCas13a	LbuCas13a	5.04	0.65343
	LshCas13a	6.84	0.49556
LbuCas13a	LbaCas13a	5.04	0.74725
	LshCas13a	6.45	0.58703
LshCas13a	LbaCas13a	6.84	0.65273
	LbuCas13a	6.45	0.68301

Table 2 Functional amino acids with high and medium scores predicted by InterProSurf server

	LbaCas13a	LshCas13a
High probability functional residues	110, 111, 112, 113, and 114	860, 861, 863, 864, 865, 866, 867, 857, 858, 1215, 1216, 1217, and 1218
Medium probability functional residues	114, 45, 115, 116, and 117	1218, 1235, 1236, 1242, 1243, 1244, 901, 903, 904, 905, 906, 907, and 1054
High probability RED stick, medium probability GREEN stick representation	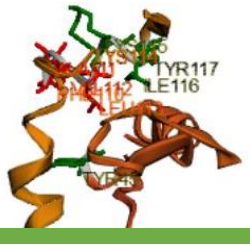	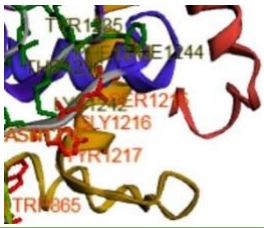

In alignment with the objectives of this investigation, structural analysis distinguished binding sites by their relatively shallow pocket morphology, while deeper pocket conformations were operationally defined as putative active sites within the protein architecture. For LbaCas13a pockets 2-5; for LbuCas13a, pockets 3-5; and for LshCas13a pockets 2, 3, and 5 were considered as binding sites. A 3D view of pockets predicted by GHECOM based on pocketness color is shown in Figure 5.

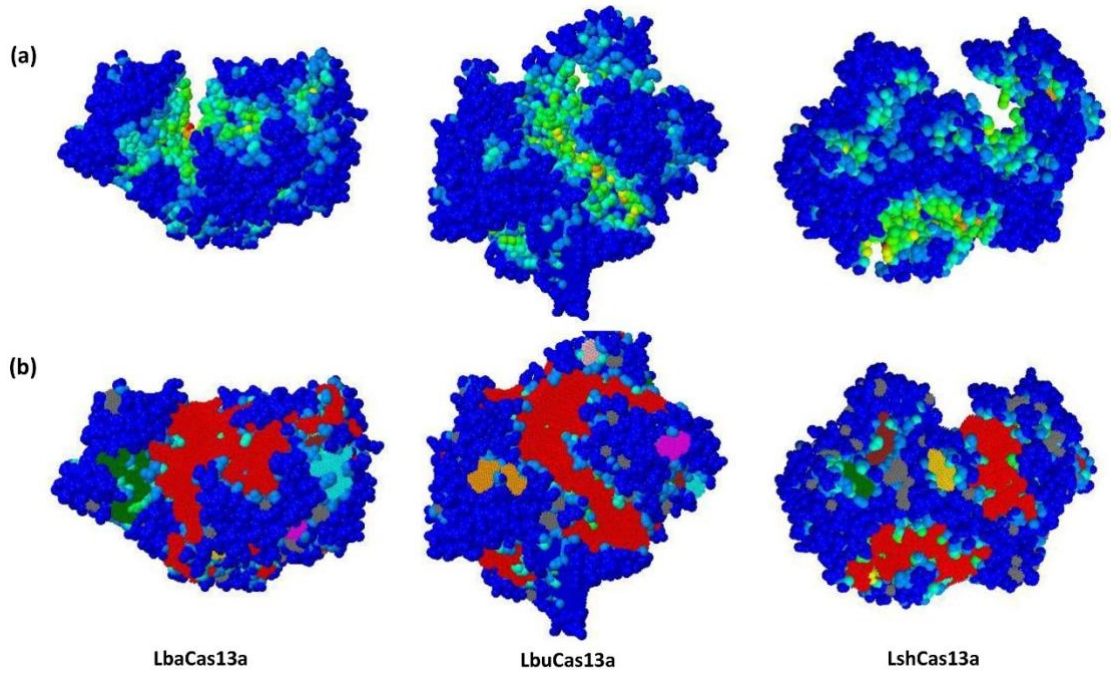

Figure 5 3D view of pocket structure predicted by GHECOM server based on (a) pocketness color and (b) cluster color. The color of pocketness bar indicates the cluster number of pockets: red for cluster 1; blue for cluster 2; green for cluster 3; yellow for cluster 4; and cyan for cluster 5

Ligand Binding Site Prediction

The potential binding sites (PBS) of proteins are those residues or atoms that bind to ligands directly on protein surface; they are near to the ligand binding sites. The potential binding sites of LbaCas13a are A: 691-695, 697-700, 705, 709, 856, 863-868, and 869 with the highest score (0.87485). The potential binding sites of LbuCas13a, are A: 877, 1063, 1065, 1103, 1105-1107, 1109-1112, 1145, 1146, 1149, 1151, and 1153, with the highest score (0.50163). The potential binding sites of LshCas13a, predicted by the eF-seek server, are A: 343, 344, 346, 347, 349, 352, 491, 494-498, and 1208 with the highest score (0.91673). Binding residues with scores higher than 0.5 predicted by eF-seek are shown in Table 3. eF-seek predictions are shown in Figure 6.

Further Scrutiny

Cas13a exhibits a predominantly α-helical structure composed of multiple distinct domains that collectively envelop the crRNA, forming an active surveillance complex. Like other single-protein CRISPR effectors, its architecture is divided into two primary lobes: the crRNA recognition (REC) lobe, which includes the N-terminal domain (NTD) and the Helical-1 domain, and the nuclease (NUC) lobe, which comprises the HEPN1, Helical-2, Helical-3, and HEPN2 domains [6,24,25]. The overall structure of the LbaCas13a, LbuCas13a, and LshCas13a complexes is shown in Figure 7.

To consolidate the findings for subsequent docking studies, the results from multiple computational tools, specifically GHECOM and eF-seek, were cross-referenced. The common regions identified across these tools were prioritized as high-confidence binding sites.

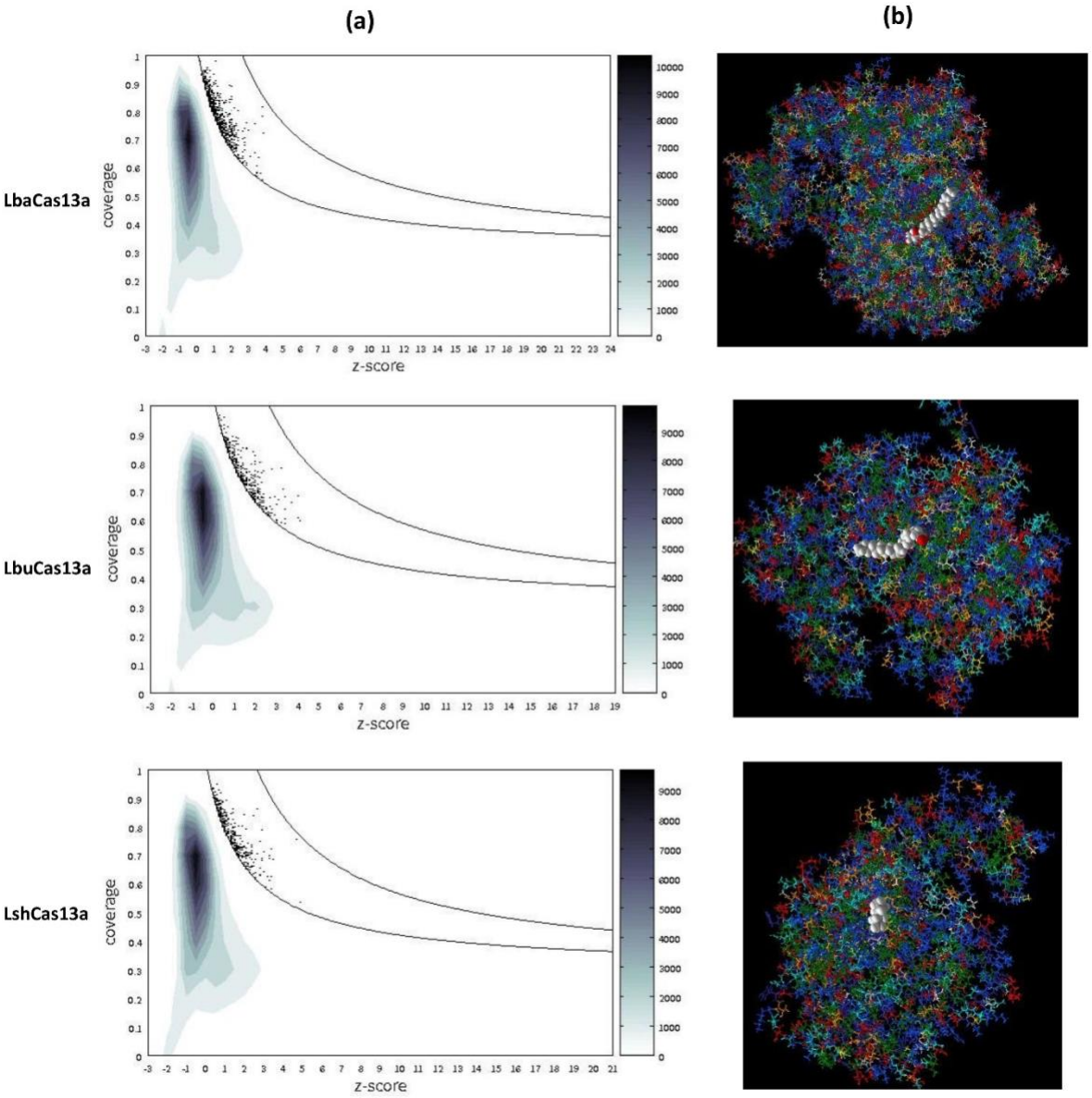

Figure 6 eF-seek predictions. (a)The density plots are illustrated. Dots in the upper right regions indicate “significantly” similar binding sites, while the lower left region indicates the non-similar binding sites. The points above the line in the density plot, which indicate the "significant" match, with the higher score highlighted in blue. (b) The complex structure of the results is shown for LbaCas13a, LbuCas13a, and LshCas13a

For LbaCas13a in the pocket 4 region, residues 603, 605, and 606 were consistently predicted as strong binding determinants. In the case of LbuCas13a, also in the pocket 4 region, residues 1112 and 1145 emerged as key mediators of ligand interactions. For LshCas13a in the pocket 5 region, residues 735, 784, and 787 were consistently flagged as active-site contributors.

Discussion

The Cas13a family exhibits a bilobed architecture consisting of REC lobe (Recognition lobe), contains Helical-1 and Helical-2 domains critical for crRNA binding and NUC lobe (Nuclease lobe), which houses HEPN domains responsible for RNase activity [24].

Table 3 The results retrieved from eF-seek are presented, with only those scoring above 0.5 being displayed

Ligand	Binding residues	Z-score	Coverage	Score
	LbaCas13a			
OLC	A: 877, 1063, 1065, 1103, 1105, 1107, 1109, 1112, 1145, 1146, 1149, 1151, and 1153	3.8	0.814	0.87485
TRD	A: 603, 606, 607, 612-614, 617, 692, 695, and 696	3.8	0.782	0.77117
TRD	A: 877, 1063, 1065, 1066, 1103, 1107, 1109, 1112, 1146, 1149, 1151, 1152, 1153	3.9	0.723	0.603
OLB	A: 873, 876, 879, 881, 1063, 1065, 1103, 1111, 1113, 1142, 1145, 1146, 1149-1152, and 1153	3.4	0.755	0.57962
HEX	A: 546, 548-550, 605, 606, 609-611, 649, 650, 652, and 653	2	0.887	0.51287
	LbuCas13a			
OLA	A: 877, 1063, 1065, 1103, 1105-1107, 1109-1112, 1145, 1146, 1149, 1151, and 1153	3.2	0.782	0.60665
TRD	A: 603, 606, 607, 612-614, 617, 692, 695, and 696	4	0.686	0.50163
	LshCas13a			
TRD	A: 343, 344, 346, 347, 349, 352, 491, 494-498, and 1208	4.7	0.755	0.91673
HEX	A: 735, 738, 739, 779, 780, 783, 784, and 787	2.7	0.863	0.68235
C8E	A: 372, 375, 376, 378-382, 463-465, and 468	2.9	0.787	0.53815

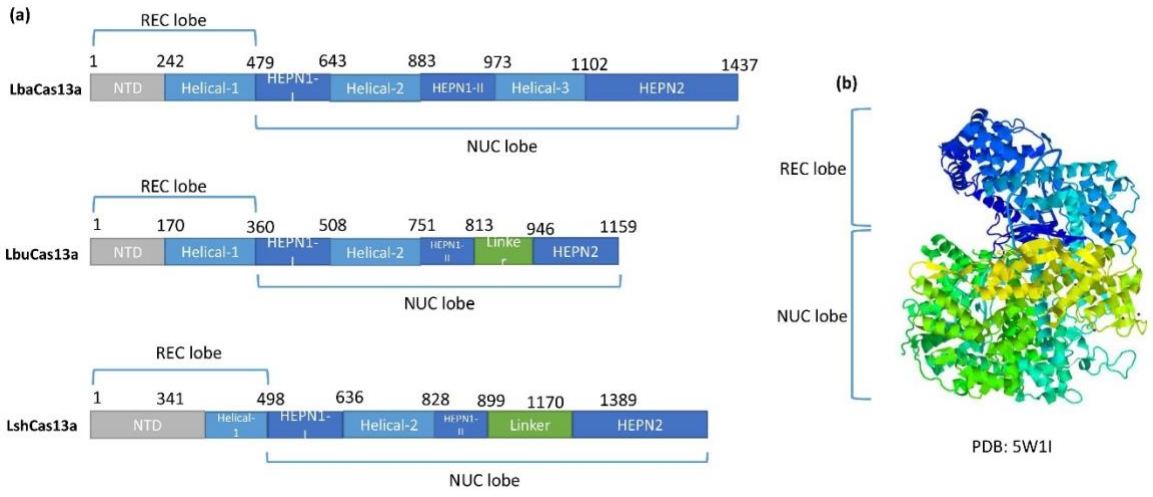

Figure 7 Overall structure of the Cas13a variants. (a) Domain organization schematic of LbaCas13a shown with the REC and NUC lobes annotated. (b) LbaCas13a: crRNA complex is shown as cartoon representation

Trans-cleavage activation occurs through a conformational change upon target RNA binding, exposing the HEPN active sites [26]. The identification and characterization of binding sites in Cas13a orthologs—LbuCas13a, LbaCas13a, and LshCas13a—require a multifaceted bioinformatic pipeline to elucidate structural features that can be modulated for improved trans-cleavage activity. Computational tools such as InterProSurf, GHECOM, and eF-seek provide complementary insights into protein-ligand interactions, cryptic binding pockets, and allosteric communication networks.

InterProSurf is instrumental in mapping solvent-accessible regions and identifying potential binding interfaces [27]. For Cas13a proteins, this tool helps delineate conserved residues involved in crRNA binding, target RNA recognition, and HEPN domain dimerization. For instance, the REC-NUC lobe hinge region in Cas proteins exhibits a high propensity for ligand binding due to its dynamic nature, as evidenced by molecular dynamics simulations [27,28]. The server identified amino acids 110 to 117 of REC lobe with high and medium probability as functional residues for LbaCas13a and some residues in NUC lobes for LshCas13a.

GHECOM (Grid-based HECOMi) employs a grid-based approach to detect buried cavities that may not be apparent in static crystal structures [29,30]. Applying GHECOM to Cas13a variants reveals several cryptic pockets adjacent to functional domains. These pockets, often overlooked in traditional docking studies, could serve as allosteric regulatory sites. Volume derived from GHECOM helps prioritize pockets for virtual screening campaigns, particularly for small molecules that could enhance trans-cleavage by stabilizing the open conformation of the HEPN domains.

The eF-seek server employs elastic network models and perturbation-response scanning to identify allosteric pathways connecting distal functional sites [31-33]. In Cas13a proteins, eF-seek analysis reveals key communication routes between the crRNA-binding region and the catalytic HEPN domains. Notably, LbaCas13a exhibits a more robust allosteric network compared to LbuCas13a and LshCas13a, which may explain its higher basal trans-cleavage activity.

By analyzing the data collected from all servers and cross-comparing the results, functional amino acids were identified across different Cas13a variants. Specifically, for LbaCas13a, amino acids 603, 605, and 606 were pinpointed; for LbuCas13a, amino acids 1112 and 1145; and for LshCas13a, amino acids 735, 784, and 787 were identified as ligand-binding sites. These residues are situated within the nuclease lobe in all three proteins. In the case of LbaCas13a and LbuCas13a, the identified amino acids are located in the HEPN domain, which is crucial for the RNase activity of Cas13a [20,24]. Modifying these residues or their interactions with small molecules could potentially enhance trans-cleavage activity by improving the catalytic efficiency or stability of the enzyme. However, further structural analyses and experimental validations are essential to confirm their precise roles and mechanisms [34-37].

Conclusion

In summary, the synergistic application of InterProSurf, GHECOM, and eF-seek provides a robust framework for identifying and optimizing binding sites in Cas13a proteins. These bioinformatic approaches not only guide experimental validation, but also accelerate the development of chemically enhanced

CRISPR-Cas13 systems for precision diagnostics and therapeutics.

Acknowledgments

The author would like to sincerely acknowledge Alzahra University for providing an outstanding academic and research environment that facilitated this study.

ORCID

Zahra Ghanei
https://orcid.org/0000-0003-0899-7688

References

[1]. Makarova, K.S., Haft, D.H., Barrangou, R., Brouns, S.J., Charpentier, E., Horvath, P., Moineau, S., Mojica, F.J., Wolf, Y.I., Yakunin, A.F., Evolution and classification of the Crispr–Cas systems. *Nature Reviews Microbiology*, **2011**, 9(6), 467-477.

[2]. Zhou, W., Hu, L., Ying, L., Zhao, Z., Chu, P.K., Yu, X.F., A CRISPR–Cas9-triggered strand displacement amplification method for ultrasensitive DNA detection. *Nature Communications*, **2018**, 9(1), 5012.

[3]. Koonin, E.V., Makarova, K.S., Zhang, F., Diversity, classification and evolution of CRISPR-Cas systems. *Current Opinion in Microbiology*, **2017**, 37, 67-78.

[4]. Makarova, K.S., Koonin, E.V., Annotation and classification of CRISPR-Cas systems. *CRISPR: Methods and Protocols*, **2015**, 47-75.

[5]. Li, Y., Li, S., Wang, J., Liu, G., Crispr/cas systems towards next-generation biosensing. *Trends in Biotechnology*, **2019**, 37(7), 730-743.

[6]. Knott, G.J., East-Seletsky, A., Cofsky, J.C., Holton, J.M., Charles, E., O'Connell, M.R., Doudna, J.A., Guide-bound structures of an rna-targeting a-cleaving crispr–cas13a enzyme. *Nature Structural & Molecular Biology*, **2017**, 24(10), 825-833.

[7]. Kick, L.M., Von Wrisberg, M.K., Runtsch, L.S., Schneider, S., Structure and mechanism of the RNA dependent RNase Cas13a from rhodobacter capsulatus. *Communications Biology*, **2022**, 5(1), 71.

[8]. Kang, B., Zhang, J., Schwoerer, M.P., Nelson, A.N., Schoeman, E., Guo, A., Ploss, A., Myhrvold, C., Highly multiplexed MRNA quantitation with Crispr-Cas13. *BIORXIV*, **2023**.

[9]. Thakku, S.G., Ackerman, C.M., Myhrvold, C., Bhattacharyya, R.P., Livny, J., Ma, P., Gomez, G.I., Sabeti, P.C., Blainey, P.C., Hung, D.T., Multiplexed detection of bacterial nucleic acids using cas13 in droplet microarrays. *PNAS Nexus*, **2022**, 1(1), pgac021.

[10]. Kaminski, M.M., Abudayyeh, O.O., Gootenberg, J.S., Zhang, F., Collins, J.J., Crispr-based diagnostics. *Nature Biomedical Engineering*, **2021**, 5(7), 643-656.

[11]. Wei, C., Lei, X., Yu, S., Multiplexed detection strategies for biosensors based on the crispr-cas system. *ACS Synthetic Biology*, **2024**, 13(6), 1633-1646.

[12]. Deng, F., Li, Y., Li, B., Goldys, E.M., Increasing trans-cleavage catalytic efficiency of Cas12a and Cas13a with chemical enhancers: Application to amplified nucleic acid detection. *Sensors and Actuators B: Chemical*, **2022**, 373, 132767.

[13]. Liu, L., Li, X., Ma, J., Li, Z., You, L., Wang, J., Wang, M., Zhang, X., Wang, Y., The molecular architecture for RNA-guided RNA cleavage by Cas13a. *Cell*, **2017**, 170(4), 714-726. e710.

[14]. Lopina, O.D. Enzyme inhibitors and activators. *Enzyme Inhibitors and Activators*, **2017**.

[15]. Dong, D., Ren, K., Qiu, X., Zheng, J., Guo, M., Guan, X., Liu, H., Li, N., Zhang, B., Yang, D., The crystal structure of cpf1 in complex with CRISPR RNA. *nature*, **2016**, 532(7600), 522-526.

[16]. Koh, Y., Yahayu, M., Ramli, S., Hanapi, S., Dailin, D., Lim, E., El Enshasy, H., Recent development in biological production of 1, 3-propanediol. *Chemical Methodologies*, **2024**, 8(6), 439-461.

[17]. National Center for Biotechnology Information. (n.d.). *Protein*. Retrieved **2025**
[18]. National Center for Biotechnology Information. (n.d.). *BLAST: Basic Local Alignment Search Tool*. Retrieved **2025**
[19]. Kiefer, F., Arnold, K., Künzli, M., Bordoli, L., & Schwede, T. The SWISS-MODEL Repository and associated resources. *Nucleic acids research*, **2009**, 37(suppl_1), D387-D392.
[20]. Zhang, Y., & Skolnick, J. TM-align: a protein structure alignment algorithm based on the TM-score. *Nucleic acids research*, **2005**, 33(7), 2302-2309.
[21]. Negi, S. S., Schein, C. H., Oezguen, N., Power, T. D., & Braun, W. InterProSurf: a web server for predicting interacting sites on protein surfaces. *Bioinformatics*, **2007**, 23(24), 3397-3399.
[22]. Osaka University. (n.d.). Ghecom: Grid-based HECOMi finder.
[23]. Kinoshita, K., Murakami, Y., & Nakamura, H. eF-seek: prediction of the functional sites of proteins by searching for similar electrostatic potential and molecular surface shape. *Nucleic acids research*, **2007**, 35(suppl_2), W398-W402.
[24]. Sponer, J., Bussi, G., Krepl, M., Banáš, P., Bottaro, S., Cunha, R.A., Gil-Ley, A., Pinamonti, G., Poblete, S., Jurecka, P., RNA structural dynamics as captured by molecular simulations: A comprehensive overview. *Chemical reviews*, **2018**, 118(8), 4177-4338.
[25]. Stella, S., Alcon, P., Montoya, G., Class 2 CRISPR–CAS RNA-guided endonucleases: Swiss army knives of genome editing. *Nature Structural & Molecular Biology*, **2017**, 24(11), 882-892.
[26]. Chen, J.S., Doudna, J.A., The chemistry of Cas9 and its CRISPR colleagues. *Nature Reviews Chemistry*, **2017**, 1(10), 0078.
[27]. Anantharaman, V., Makarova, K.S., Burroughs, A.M., Koonin, E.V., Aravind, L., Comprehensive analysis of the HEPN superfamily: Identification of novel roles in intra-genomic conflicts, defense, pathogenesis and RNA processing. *Biology Direct*, **2013**, 8(1), 15.
[28]. Yoon, P.H., Zhang, Z., Loi, K.J., Adler, B.A., Lahiri, A., Vohra, K., Shi, H., Rabelo, D.B., Trinidad, M., Boger, R.S., Structure-guided discovery of ancestral crispr-cas13 ribonucleases. *Science*, **2024**, 385(6708), 538-543.
[29]. Liu, X., Kang, X., Lei, C., Ren, W., Liu, C., Programming the trans-cleavage activity of crispr-cas13a by single-strand DNA blocker and its biosensing application. *Analytical Chemistry*, **2022**, 94(9), 3987-3996.
[30]. Negi, S.S., Schein, C.H., Oezguen, N., Power, T.D., Braun, W., InterProSurf: A web server for predicting interacting sites on protein surfaces. *Bioinformatics*, **2007**, 23(24), 3397-3399.
[31]. Saha, A., Arantes, P.R., Hsu, R., Narkhede, Y.B., Jinek, M., Palermo, G., Cooperative dynamics of rec-nuc lobes prime CAS12A for DNA processing. *Biophysical Journal*, **2021**, 120(3), 16a-17a.
[32]. Payacán Ortiz, C.V. A non-integrative Crispr/Cas9 genome-editing approach for use in vegetable crop breeding. **2022**.
[33]. Kawabata, T., Detection of multiscale pockets on protein surfaces using mathematical morphology. *Proteins: Structure, Function, and Bioinformatics*, **2010**, 78(5), 1195-1211.
[34]. Zhang, Z., Li, Y., Lin, B., Schroeder, M., Huang, B., Identification of cavities on protein surface using multiple computational approaches for drug binding site prediction. *Bioinformatics*, **2011**, 27(15), 2083-2088.
[35]. Kinoshita, K., Murakami, Y., Nakamura, H., Ef-seek: Prediction of the functional sites of proteins by searching for similar electrostatic potential and molecular surface shape. *Nucleic acids research*, **2007**, 35(suppl_2), W398-W402.
[36]. Viet Hung, L., Caprari, S., Bizai, M., Toti, D., Polticelli, F., Libra: Ligand binding site recognition application. *Bioinformatics*, **2015**, 31(24), 4020-4022.

[37]. He, Q.F., Li, D., Xu, Q.Y., Zheng, S., Predicted essential proteins of plasmodium falciparum for potential drug targets. *Asian Pacific Journal of Tropical Medicine*, **2012**, 5(5), 352-354.

How to cite this article:
Z. Ghanei, Structural Insights and Binding Site Analysis for Improved CRISPR-Cas13a Sensitivity and Efficiency. *International Journal of Advanced Biological and Biomedical Research*, 2026, 14(1), 90-103.
DOI: https://doi.org/10.48309/ijabbr.2026.2065708.1635
Link: https://www.ijabbr.com/article_730088.html